

# Genetic robustness of let-7 miRNA sequence-structure pairs

Qijun He<sup>1</sup>, Fenix W. Huang<sup>1</sup>, Christopher Barrett<sup>1,4</sup> and Christian M. Reidys<sup>1,2,3\*</sup> \*

<sup>1</sup> Biocomplexity Institute of Virginia Tech, Blacksburg, VA, USA. <sup>2</sup> Department of Mathematics, Virginia Tech, Blacksburg, VA, USA. <sup>3</sup> Thermo Fisher Scientific Fellow in Advanced Systems for Information Biology. <sup>4</sup> Department of Computer Science, Virginia Tech, Blacksburg, VA, USA.

## ABSTRACT

Genetic robustness, the preservation of evolved phenotypes against genotypic mutations, is one of the central concepts in evolution. In recent years a large body of work has focused on the origins, mechanisms, and consequences of robustness in a wide range of biological systems. In particular, research on ncRNAs studied the ability of sequences to maintain folded structures against single-point mutations. In these studies, the structure is merely a reference. However, recent work revealed evidence that structure itself contributes to the genetic robustness of ncRNAs. We follow this line of thought and consider sequence-structure pairs as the unit of evolution and introduce the spectrum of inverse folding rates (IFR-spectrum) as a measurement of genetic robustness. Our analysis of the miRNA let-7 family captures key features of structure-modulated evolution and facilitates the study of robustness against multiple-point mutations.

## INTRODUCTION

Genetic robustness can be characterized in terms of the variation of phenotype distribution induced by genotypic change (1, 2, 3) and concerns the insensitivity of a phenotype to genetic changes. Mutational robustness has been studied in the context of noncoding RNA (ncRNA) (4, 5). RNA consists of a single strand of nucleotides (A,C,G,U) that can fold and bond to itself through base pairing. ncRNAs are known to function in aptamer binding as riboswitches, in chemical catalysis as ribozymes and in RNA splicing such as spliceosome (6, 7, 8, 9). Most importantly, it is the folded structure that is underlying all these mechanisms, allowing for the interaction with and subsequent modification of other biological molecules. The self folding of RNA makes it an ideal object to study genotype-phenotype relations. The well-established energy based prediction of RNA secondary structure, a 2-dimensional coarse grain of the real three dimensional structure, makes such studies feasible (10, 11, 12, 13).

Structures are an important determinant of the function of ncRNAs, whence the robustness of an RNA can be characterized in terms of the variation of secondary structure distribution, i.e. the stability of a secondary structure in the face of genetic sequence changes. Structural robustness of ncRNAs is considered to be a key component of the fitness of the molecule and much research has been conducted

to identify the footprints of natural selection on secondary structures of sncRNAs (4, 5). In (4), Borenstein and Ruppin define neutrality of an RNA sequence  $\sigma = a_1 a_2 \dots a_n$  by  $\eta(\sigma) = 1 - \langle d \rangle / n$ , where  $\langle d \rangle$  denotes the average, taken over all  $3n$  single-point mutants of  $\sigma$ , of the base pair distance  $d$  between the minimum free energy (MFE) structure,  $S_0$ , of  $\sigma$  and the MFE structures of single-point mutants. The RNA sequence,  $\sigma$ , is then defined to be robust if  $\eta(\sigma)$  is greater than the average neutrality of 1000 control sequences generated by the program RNAinverse (14), which fold into the same target structure,  $S_0$ . The main finding of (4) is that precursor miRNAs (pre-miRNA) exhibit a significantly higher level of mutational robustness than random RNA sequences, having the same structure. Subsequently Rodrigo et al. (5) undertook a similar analysis for bacterial small RNAs. Their main finding was, that, surprisingly, bacterial sncRNAs are not significantly more robust when compared with 1000 sequences having the same structure, as computed by RNAinverse. (5) based their findings on the notion of *ensemble diversity* defined earlier in (15).

In the above mentioned papers, robustness is defined by taking the average of all  $3n$  single-point mutants, the underlining assumption being, that all  $3n$  single-point mutations are equally likely to occur and, in addition, taking exclusively single-point mutations into account. Incorporation of multiple-point mutations poses obvious difficulties, since the number of sequences that need to be taken into consideration will grow exponentially.

The neutral theory of Motoo Kimura (16), stipulates that evolution is achieved by neutral mutations, that is, by mutations, that are necessarily compatible with the underlying structure. This is in accordance with recent findings showing that secondary structures have a *genuine* influence on selection in RNA genes. In (17), Hein *et al.* classify stem positions into structural classes and validate that they are under different selective constraints. In (18), the authors observe neutral evolution in *Drosophila* miRNA and evolution increasing the thermal dynamic stability of the RNA. (19, 20) study Human Accelerated Regions (HAR) in brains of primates, i.e. noncoding RNAs with an accelerated rate of nucleotide substitutions along the lineage between human and chimpanzee. (20) concludes that this increased rate of nucleotide substitutions is of central importance for the evolution of the human brain. The most divergent of these regions, HAR1, has been biochemically confirmed to

\*To whom correspondence should be addressed. Tel: +01 540 231-2317; Email: duckcr@bi.vt.edu

fold into distinct RNA secondary structures in human and chimpanzee. Interestingly, the mutations in the human HARI sequence, compared to the chimpanzee sequence, stabilize their respective RNA structure (21), suggesting a shape modulated evolution.

Recently, (22) proposed a framework considering RNA sequences and their RNA secondary structures simultaneously. This gives rise to an information theoretic framework for RNA sequence-structure pairs. In particular, the authors studied the “dual Boltzmann distribution”, i.e. the Boltzmann distribution of sequences with respect to a fixed structure. The authors develop a Boltzmann sampler of sequences with respect to a given structure and study the “inverse folding rate” (IFR) of the sampled sequences, i.e. the proportion of the sampled sequences whose MFE structure equals to the given structure. (22) reports that natural structures have higher IFR than random structures, suggesting that natural structures have higher intrinsic robustness than random structures.

This suggests an approach to consider sequences and structures-as *pairs*-as the unit of evolution, instead of just sequences in isolation. In this paper, we generalize the notion of *inverse folding rate* (IFR) and introduce a novel profile, the *IFR-spectrum*, of a sequence-structure pair. By construction, this spectrum entails both sequence and structure information. The key idea is that mutations will be biased by the underlying thermodynamic energy of the respective structure, instead of being equally likely to occur.

We shall conduct a detailed study on the let-7 family miRNAs, small endogenous noncoding RNAs, that regulate the expression of protein coding genes in animals. The short, mature miRNAs (~22 nt) originate from longer RNA precursor molecules that fold into a stem-loop hairpin structure. The secondary structure of miRNA stem-loops serves a crucial role in the miRNA gene maturation process (23). The stem-loop structure has been under evolutionary pressures to conserve its structure. Such stabilizing pressures favor robust configurations and may have led to the evolution of robust structures. Furthermore, the let-7 miRNA family has been widely detected in metazoans, ranging from human to fruit fly (24). These features make the let-7 gene family a particularly suitable test bed for studying the evolution of genetic robustness.

We organize our study as follows: first we shall extend the analysis of (4) to IFR-spectra and observe that most native sequence-structure pairs have a higher IFR-spectrum than sequence-structure pairs obtained by the inverse folding algorithm. We shall investigate different aspects of the robustness of IFR-spectra of native sequence-structure pairs and show that these are distinctively more robust against multiple-point mutations. Secondly, we conduct cross-species comparisons of native sequence-structure pairs, observing that higher metazoan species have higher IFR-spectra. Our analysis suggests that IFR-spectra are being increased in the course of shape-modulated evolution.

## MATERIALS AND METHODS

### IFR-spectrum: a sequence-structure pair profile.

In this section we introduce the technical details of our framework, starting with Borenstein and Ruppin’s definition of neutrality (4), as the average of all  $3n$  single-point mutants. By construction, all mutations are equivalent and structure has no influence on the mutation rate. However, as suggested in (17, 18, 21), structure genuinely affects mutation rate and mutations in turn further increase the thermal dynamic stability of the structure. We consider here mutations with respect to a *fixed* structure and consequently deal exclusively with *compatible* mutations. Furthermore, the idea of the following is to favor energetically beneficial mutations, while penalizing detrimental mutations. To adequately quantify the above, we revisit some of the basic concepts of the thermodynamic model of RNA secondary structure.

The free energy  $\eta$  can be considered as a result of pairing sequences and structures as follows:

$$\eta: \mathcal{Q}_4^n \times \mathcal{S}_n \rightarrow \mathbb{R} \sqcup +\infty,$$

where  $\mathcal{Q}_4^n$  and  $\mathcal{S}_n$  denote the space of sequences,  $\sigma$ , and the space of secondary structures,  $S$ , respectively and  $\eta(\sigma, S)$  is the energy of  $S$  on  $\sigma$ . This mapping is computed as the sum of the energy contributions of individual base-pairs (25). A more elaborate model (11, 26) evaluates the total free energy to be the sum of from the energies of loops involving multiple base-pairs. We remark that, if a sequence,  $\sigma$ , is not compatible with a structure,  $S$ , then  $\eta(\sigma, S) = +\infty$ . Then MFE-folding is a map from sequences to distinguished structures, i.e. the minimum free energy structures:

$$\text{mfe}: \mathcal{Q}_4^n \rightarrow \mathcal{S}_n, \quad \sigma \mapsto \underset{S \in \mathcal{S}_n}{\text{argmin}} \eta(\sigma, S).$$

To incorporate the thermodynamic information into the probability of mutations, we introduce the notion of the Boltzmann distribution of  $k$ -point mutants of a sequence-structure pair. To this end, we consider the partition function of  $k$ -point mutants of a sequence-structure pair, namely, the partition function of all sequences that are at Hamming distance  $k$  to the given sequence with respect to the given structure.

**DEFINITION 1.** *Let  $\sigma$  be a sequence of  $n$  nucleotides and let  $S$  be its associated structure, i.e. its MFE- or native structure. Then the partition function of  $k$ -point mutants of  $\sigma$  with respect to  $S$  is given by:*

$$Q_{\sigma,k}^S = \sum_{\sigma', h(\sigma, \sigma')=k} e^{-\frac{\eta(\sigma', S)}{RT}}, \quad (1)$$

where  $h$  is the Hamming distance,  $\eta(\sigma', S)$  is the energy of  $S$  on  $\sigma'$ ,  $R$  is the universal gas constant and  $T$  is the temperature.

Eq. (1) represents the “dual” of McCaskill’s partition function (27) with an additional Hamming distance filtration (28). Given this partition function, we are in position to

introduce the *Boltzmann distribution* of  $k$ -point mutants of  $\sigma$  with respect to  $S$ : the probability of a specific  $k$ -point mutant  $\sigma^*$  of  $\sigma$ ,  $h(\sigma^*, \sigma) = k$ , with respect to  $S$ :

$$Pr_{\sigma,k}^S(\sigma^*) = \frac{e^{-\frac{\eta(\sigma^*, S)}{RT}}}{Q_{\sigma,k}^S}.$$

This expression allows us to consider Boltzmann weighted mutations, taking into account the free energy, when realizing  $S$ .

In order to quantify mutational robustness, i.e. the ability to maintain the structure, we consider all  $k$ -point mutants, that fold again into  $S$ . We call the fraction of  $k$ -point mutants,  $\sigma^*$ , that fold into  $S$ , the *inverse folding rate* (IFR) of the sequence structure pair  $(\sigma, S)$  at  $k$ , that is, we have

$$\text{IFR}_{\sigma,k}^S = \sum_{\text{mfe}(\sigma^*)=S} Pr_{\sigma,k}^S(\sigma^*).$$

$\text{IFR}_{\sigma,k}^S$  thus quantifies the mutational robustness of a sequence-structure pair,  $(\sigma, S)$ , with respect to Boltzmann weighted  $k$ -point mutations, taking into account the energy of the sequence, when assuming the structure  $S$ .

$\text{IFR}_{\sigma,1}^S$  can be viewed as a variation of Borenstein and Ruppin’s definition of neutrality. Instead of a uniform distribution of all  $3n$  single-point mutants, a Boltzmann weighted distribution for these mutants is employed. In contrast to using base pair distance as the metric on structure space, we restrict ourselves to a discrete metric.

The *IFR $_{\sigma,k}^S$ -spectrum* of a sequence-structure pair,  $(\sigma, S)$ , i.e. the collection of  $\text{IFR}_{\sigma,k}^S$  for varying  $k$ , allows us to study multiple-point mutations instead of confining the analysis to single-point mutations. In this study, we shall analyze the *IFR $_{\sigma,k}^S$ -spectrum* of sequence-structure pairs of Hamming distances  $1 \leq k \leq 20$ .

The *IFR $_{\sigma,k}^S$ -spectrum* can be viewed as the conditional probability of the IFR in (22), conditional to specific Hamming distances. As a result, we have:

$$\text{IFR}^S = \sum_{k=0}^n Pr_{\sigma}^S(k) \text{IFR}_{\sigma,k}^S,$$

where  $Pr_{\sigma}^S(k) = \frac{Q_{\sigma,k}^S}{Q^S}$ ,  $Q^S = \sum_{\sigma'} e^{-\frac{\eta(\sigma', S)}{RT}}$ .

### The *IFR $_{\sigma,k}^S$ -spectrum* via Boltzmann sampling.

Computing  $\text{IFR}_{\sigma,k}^S$  strictly requires folding all  $\sigma'$  that are  $S$ -compatible, such that  $h(\sigma, \sigma') = k$ . While this task is impractical for large  $k$ ,  $\text{IFR}_{\sigma,k}^S$  can be efficiently computed by means of Boltzmann sampling. This is conducted here via the Hamming Distance Restricted Dual Sampler (HRDS) (28), which facilitates the approximation of  $\text{IFR}_{\sigma,k}^S$  for any given sequence-structure pair,  $(\sigma, S)$ , and Hamming distance,  $k$ . HDRS takes as input  $(\sigma, S)$  and  $k$  and outputs sequences,

$\sigma^*$ , having Hamming distance  $k$  with probability  $\frac{e^{-\frac{\eta(\sigma^*, S)}{RT}}}{Q_{\sigma,k}^S}$ .

We then have:

$$\text{IFR}_{\sigma,k}^S \approx \frac{\# \text{ of sequences folding into } S}{\# \text{ of sampled sequences}}.$$

In this paper,  $\text{IFR}_{\sigma,k}^S$  is calculated by sampling 5000 sequences and computing their MFE structures. The standard error of measuring  $\text{IFR}_{\sigma,k}^S$  by sampling 5000 times is  $\pm 0.0065$  (derived by computing the  $\text{IFR}_{\sigma,5}^S$  of aae-let-7 sequence-structure pairs 100 times). By computing the  $\text{IFR}_{\sigma,k}^S$  for each  $1 \leq k \leq 20$ , we obtain the *IFR $_{\sigma,k}^S$ -spectrum* of the sequence-structure pairs,  $(\sigma, S)$ .

### miRNA data.

We consider 401 miRNA precursor sequences of the let-7 gene family, obtained from the miRBase database (29). These originate from 82 different animal species. In vertebrate and urochordates multiple homologous miRNA genes are commonly observed, while single miRNA let-7 genes were more common in other animal species. We provide in the supplemental materials (SM) the numbers of the respective let-7 genes (see Table 1 in SM). The secondary structures of these sequences are derived using a MFE folding algorithm, employing the Turner energy model (26). We compute the *IFR $_{\sigma,k}^S$ -spectrum*, for  $1 \leq k \leq 20$ , for all 401 let-7 sequence-structure pairs.

## RESULTS

### Robustness of native let-7 sequence-structure pairs.

Borenstein and Ruppin (4) report that miRNA sequences exhibit a high level of neutrality in comparison with random sequences folding into a similar structure, suggesting that native miRNA sequence are more robust against single-point mutations. These results motivate further analysis of native and random sequences, in particular whether or not this neutrality is confined to a local neighborhood. To this end we uniformly select 50 of the 401 native sequence-structure pairs of the let-7 miRNA family (see Table 2 in the SM). For each such native pair,  $(\sigma, S)$ , we derive 100 random sequences,  $\sigma^*$ , whose MFE structure is identical to  $S$ , as control set. These control sequences are computed using the inverse folding algorithm presented in (22, 30, 31). Given structure  $S$ , we compute the partition function of all sequences with respect to  $S$ . We then Boltzmann sample sequences and filter (by rejection) those sequences, that fold into  $S$ . We then compute the *IFR $_{\sigma^*,k}^S$ -spectrum* for the inverse folding solutions and compare for each native sequence-structure pair  $(\sigma, S)$ , the *IFR $_{\sigma,k}^S$ -spectrum* with  $\mu(\text{IFR}_{\sigma^*,k}^S)$ -spectrum, i.e. the mean of all 100 spectra,  $\text{IFR}_{\sigma^*,k}^S$ , taken at each respective  $k$ . We call  $(\sigma, S)$   $k$ -robust, if  $\text{IFR}_{\sigma,k}^S > \mu(\text{IFR}_{\sigma^*,k}^S)$ . We then check the native sequence-structure pairs for  $k$ -robustness and quantify the significance of  $k$ -robustness via  $Z$ -tests. In Figure 1 we depict a sequence-structure pair, that is  $k$ -robust for  $1 \leq k \leq 20$ .

4 Nucleic Acids Research, , Vol. , No.

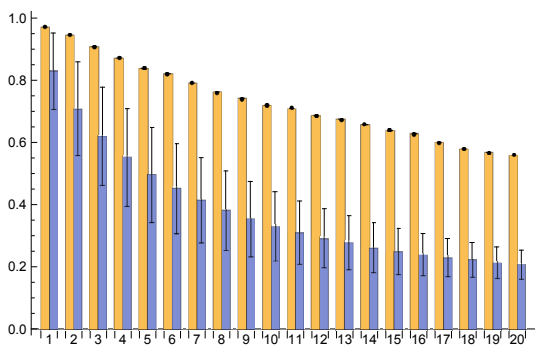


**Figure 1.** The  $IFR_{\sigma,k}^S$ -spectrum: the  $x$ -axis denotes the Hamming distance and the  $y$ -axis the inverse folding rate. The  $IFR_{\sigma,k}^S$ -spectrum of the api-let-7 (*Acyrtosiphon pisum*) gene (yellow) and the spectrum of means of the corresponding control set,  $\mu(IFR_{\sigma^*,k}^S)$  (blue). The error bar denotes the standard deviation of the control set of  $\{IFR_{\sigma^*,k}^S\}$  for each  $k$ . Since  $IFR_{\sigma,k}^S > \mu(IFR_{\sigma^*,k}^S)$ , api-let-7 is  $k$ -robust, for all  $1 \leq k \leq 20$ .  $IFR_{\sigma,k}^S$  decreases slower than  $\mu(IFR_{\sigma^*,k}^S)$ , as  $k$  increases.

In Table 1 we summarize the data on  $k$ -robustness of the 50 let-7 sequence-structure pairs included in our study. We observe that 96% of the selected let-7 miRNAs are 1-robust. This observation is consistent with (4), providing further evidence that native let-7 sequence-structure pairs are robust against single-point mutations. However, the mutational robustness of native let-7 sequence-structure pairs is not restricted to single-point mutations: for all  $1 \leq k \leq 20$ , we observe that  $k$ -robustness holds for over 90% of the selected sequence-structure pairs. This suggests, that the mutational robustness of let-7 sequence-structure pairs is not a local phenomenon. Furthermore, the percentage of significantly  $k$ -robust genes increases as  $k$  increase, see Table 1. In Figure 1 we display the  $IFR_{\sigma,k}^S$ -spectrum of the api-let-7 sequence-structure pair, illustrating the aforementioned phenomenon. The api-let-7 sequence-structure pair is 1-robust but not significantly 1-robust. However, for  $5 \leq k \leq 20$ , the api-let-7 sequence-structure pairs is significantly  $k$ -robust.

We proceed by considering for each native sequence-structure pair  $(\sigma, S)$ ,  $r_k$ , its  $IFR_{\sigma,k}^S$ -rank among the  $IFR_{\sigma^*,k}^S$ -values, respectively. Figure 2 presents the distribution of  $r_k$ , for  $k=1,5,20$ . Examination of the rank distribution shows

**Table 1.**  $k$ -robustness of native sequence-structure pairs

Hamming distance	$k$ -robust	$p < 0.05$
k=1	96%	8%
k=2	96%	28%
k=3	94%	38%
k=4	92%	38%
k=5	94%	38%
k=10	92%	48%
k=15	94%	56%
k=20	96%	58%

Second column: the percentage of  $k$ -robust ( $IFR_{\sigma,k}^S > \mu(IFR_{\sigma^*,k}^S)$ ) genes. Third column: the percentage of the significantly  $k$ -robust genes for  $p < 0.05$ . The  $p$  values denote the probability of observing  $IFR_{\sigma^*,k}^S > IFR_{\sigma,k}^S$  by chance and are calculated via  $Z$ -tests.

that native pairs exhibit a propensity towards high ranks for each  $k$ , supporting the observation of  $k$ -robustness. As  $k$  increases, the propensity towards high ranks becomes more and more pronounced. In case of  $k=1$ , only 4 out of 50 native sequence-structure pairs have  $r_1=1$ . For  $k=20$ , however, this quantity increases to 23. This is consistent with the increasing percentage of significantly  $k$ -robust genes as  $k$  increases, further demonstrating that native let-7 sequence-structure pairs exhibit mutational robustness against multiple-point mutations.

By comparing specific native sequence-structure pairs with the respective control pairs (obtained by inverse folding), we observe native sequence-structure pairs exhibit in general higher  $IFR_{\sigma,k}^S$ -values. In this analysis the sequence-structure pair,  $(\sigma, S)$ , is fixed and we contrast native pairs with pairs obtained via random inverse folded sequences.

We can augment this analysis by considering the *ensemble* of spectra of native pairs versus the *ensemble* of all inverse folded sequence-structure pairs. In that, for any fixed  $k$ , we can integrate the information of all native pairs contrasting this with the integrated information of the inverse folded pairs. Figure 3 displays these two distributions:  $IFR_{\sigma,k}^S$  of native pairs and  $\mu(IFR_{\sigma^*,k}^S)$ , of the inverse folded pairs for  $k=1,5,20$ . For each  $k$ , we not only observe that the mean of the  $IFR_{\sigma,k}^S$  is greater than that of the terms  $\mu(IFR_{\sigma^*,k}^S)$ , but also that the distributions of  $IFR_{\sigma,k}^S$  and  $\mu(IFR_{\sigma^*,k}^S)$  are distinctively different. Furthermore, the difference between the two distributions for each  $k$  is statistically significant, see Table 2, where the  $p$  value is calculated by two tailed Wilcoxon signed rank tests for paired data.

The increase of significantly  $k$ -robust native sequence-structure pairs for increasing  $k$ , as well as the tendency of native  $IFR_{\sigma,k}^S$ , to assume high ranks, for increasing  $k$ , suggest that  $k$ -robustness,  $2 \leq k \leq 20$ , is not a byproduct of 1-robustness.

Clearly, the very notion of  $IFR_{\sigma,k}^S$ -spectrum raises the question to what extend  $k$ -robustness of native sequence-structure pairs,  $2 \leq k \leq 20$ , is strongly correlated to 1-robustness. In other words, to what extent is robustness against multiple-point mutations induced by robustness against single-point mutations.

In order to quantify this, we conduct a systematic correlation analysis for  $IFR_{\sigma,k}^S$  and  $\mu(IFR_{\sigma^*,k}^S)$ . Regarding  $\mu(IFR_{\sigma^*,k}^S)$  as the intrinsic  $k$ -robustness of the structure  $S$ , we

**Table 2.** Distinct distribution of  $IFR_{\sigma,k}^S$  and  $\mu(IFR_{\sigma^*,k}^S)$

Hamming distance	mean $IFR_{\sigma,k}^S$	mean $\mu(IFR_{\sigma^*,k}^S)$	$p$ value
k=1	0.9118	0.7904	$1.09 \times 10^{-9}$
k=5	0.5952	0.4220	$3.57 \times 10^{-9}$
k=20	0.2483	0.1387	$2.23 \times 10^{-9}$

The second and third columns display the mean value of  $IFR_{\sigma,k}^S$  and  $\mu(IFR_{\sigma^*,k}^S)$ , respectively, for each  $k$ .  $p$  values denote the probability of observing more extreme differences between  $\{IFR_{\sigma,k}^S\}$  and  $\{\mu(IFR_{\sigma^*,k}^S)\}$  at random, assuming two samples are drawn from the same distribution. The  $p$  value is calculated by two tailed Wilcoxon signed rank test for paired data.

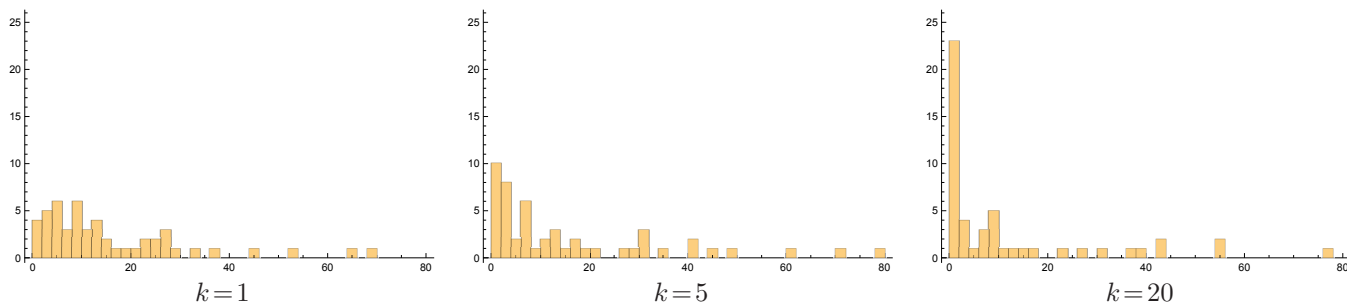


**Figure 2.** The distribution of  $IFR_{\sigma,k}^S$ -ranks,  $r_k$ , of the native sequence-structure pairs  $IFR_{\sigma,k}^S$ . The  $x$ -axis denotes ranking and the  $y$ -axis frequency,  $k=1$  (Left),  $k=5$  (Center) and  $k=20$  (Right). For each native sequence-structure pair,  $(\sigma, S)$ , the  $IFR_{\sigma,k}^S$  is ranked among 100  $IFR_{\sigma^*,k}^S$ -values, where  $\sigma^*$  is a random sequence whose MFE structure is  $S$ .

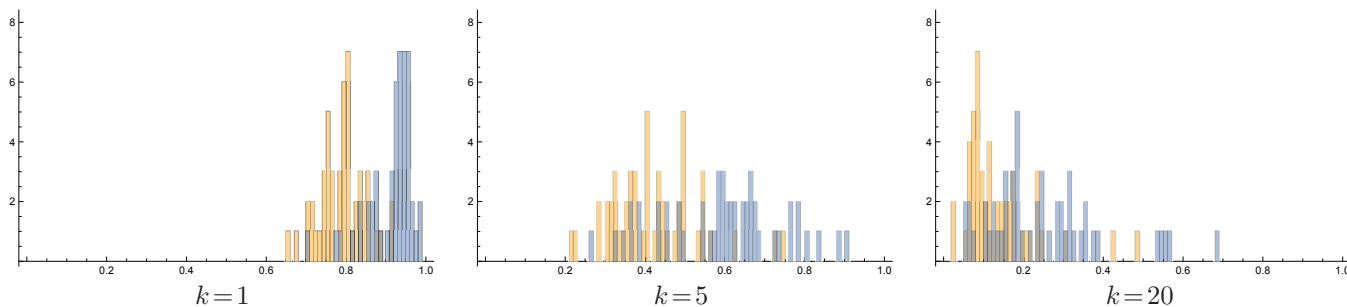


**Figure 3.** The distribution of  $IFR_{\sigma,k}^S$  of native pairs (blue) and  $\mu(IFR_{\sigma^*,k}^S)$ , of the control sets (yellow). The  $x$ -axis denotes the inverse folding rate and the  $y$ -axis denotes the frequency,  $k=1$  (Left)  $k=5$  (Center)  $k=20$  (Right).

arrive at interpreting the term  $IFR_{\sigma,k}^S - \mu(IFR_{\sigma^*,k}^S)$  as adaptive  $k$ -robustness.

The intrinsic structural  $k$ -robustness  $\mu(IFR_{\sigma^*,k}^S)$  between different  $k$  exhibits very strong correlation. Point in case: Spearman’s rank correlation coefficient between  $\mu(IFR_{\sigma^*,1}^S)$  and  $\mu(IFR_{\sigma^*,20}^S)$  is 0.8426, where  $p < 10^{-13}$ . However, the correlation between  $IFR_{\sigma,1}^S - \mu(IFR_{\sigma^*,1}^S)$  and  $IFR_{\sigma,k}^S - \mu(IFR_{\sigma^*,k}^S)$ , drops much faster as  $k$  increases. The Spearman’s rank correlation coefficient between  $IFR_{\sigma,1}^S - \mu(IFR_{\sigma^*,1}^S)$  and  $IFR_{\sigma,20}^S - \mu(IFR_{\sigma^*,20}^S)$  is 0.3693; where  $p=0.0083$ , showing weak correlation. This indicates that there exists factors beyond 1-robustness that contribute to the  $k$ -robustness of native sequence-structure pairs.

We finally study the role of the free energy for  $k$ -robustness. (32) reports that miRNA exhibits increased thermodynamic stability and furthermore that mutations in the HAR further stabilize the structure (21). This gives rise to the question whether increased  $k$ -robustness is a result of the increased thermodynamic stability of miRNAs.

To test this, we select a native sequence-structure pair from the miRNA let-7 family and generate two sets of sequences:  $\Sigma_{\text{high}}$  and  $\Sigma_{\text{low}}$ , each consisting of 30 sequences that fold into  $S$ , having higher and lower energy than the native pair, respectively. It turns out, that sequences generated by RNAinverse (14) tend to have higher energy than the native pair, while sequences generated by the dual Boltzmann sampler, filtered by rejection to fold into  $S$ , tend to have lower

energy. We compute the mean and the standard deviation of the spectra of the sequences of  $\Sigma_{\text{low}}$  and  $\Sigma_{\text{high}}$  respectively and integrate our findings in Figure 4.

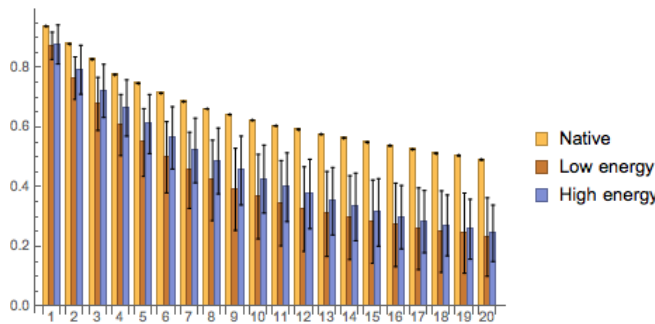


**Figure 4.** Spectra of a native sequence-structure pair versus those of inverse folding solutions having lower and higher energies. We display the spectrum of the native, let-7 miRNA pair (yellow), the spectrum of the mean  $IFR_{\sigma,k}^S$  of inverse fold solutions having lower (red) and higher (blue) energy, respectively and their standard deviations. The  $x$ -axis denotes the Hamming distance and the  $y$ -axis the inverse folding rate.

Figure 4 shows that the  $IFR_{\sigma,k}^S$ -spectrum of the native pair is distinctively higher than the ones derived from  $\Sigma_{\text{low}}$  and  $\Sigma_{\text{high}}$ . We have confirmed this result for 10 additional native sequence-structure pairs. The findings suggest that thermodynamic stability is not the sole factor, native pairs have been selected for. The mutational robustness of native

pairs is not a byproduct of evolving toward thermodynamic stability.

### Robustness of metazoan species.

(33) studies genetic robustness of networks of bacterial genes, observing variations among species in their level of genetic robustness, reflecting adaptations to different ecological niches and lifestyles. The genetic robustness of a network refers to its ability to buffer mutations via the existence of alternative pathways. The species-specific variations raise the question whether such variations can also be observed for the  $IFR_{\sigma,k}^S$ -spectra across different animal species. Are  $IFR_{\sigma,k}^S$ -spectra to some extent a reflection of phylogenetic relationships?

Herein, we perform an evolutionary analysis of the  $IFR_{\sigma,k}^S$ -spectra of let-7 miRNA sequence-structure pairs across different animal species. We first perform our analysis on 6 selected taxa: Homo sapiens, Pan paniscus, Anolis carolinensis, Ciona, Drosophila, Chromadorae. There are 12, 12, 11, 11, 14 and 7 let-7 genes found in the miRBase within each taxon, respectively. For almost all  $1 \leq k \leq 20$ , we observe the mean  $IFR_{\sigma,k}^S$ -value within each taxa to decrease from Homo sapiens to Chromadorae, see Figure 5 and Table. 3. The only exceptions are the  $IFR_{\sigma,k}^S$ -values of Pan paniscus, that become slightly larger than those of Homo sapiens, for  $14 \leq k \leq 20$ . We observe that “higher” metazoan species, as Homo sapiens, Pan paniscus, Anolis carolinensis, Ciona, all of which being Chordata, exhibit larger  $IFR_{\sigma,k}^S$ -values than “lower” metazoan species, as Drosophila, Chromadorae, all of which being Ecdysozoa. In addition, the difference of

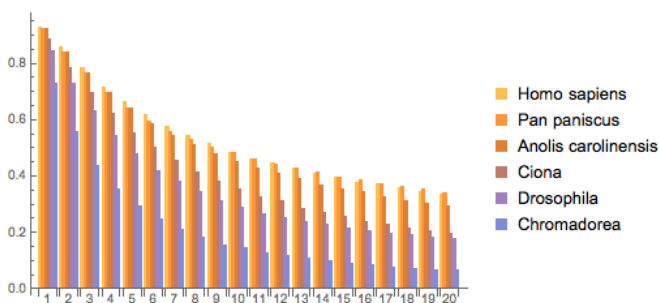


**Figure 5.** Mean  $IFR_{\sigma,k}^S$  within each of the six taxa, from left to right: Homo sapiens, Pan paniscus, Anolis carolinensis, Ciona, Drosophila, Chromadorae. The  $x$ -axis denotes the Hamming distance and the  $y$ -axis the inverse folding rate. The relative ordering of  $IFR_{\sigma,k}^S$ -values among taxa is consistent for each  $k$  (from high to low: Homo sapiens, Pan paniscus, Anolis carolinensis, Ciona, Drosophila, Chromadorae, the only exception being  $IFR_{\sigma,k}^S$ -values of Pan paniscus becoming slightly larger than those of Homo sapiens, for  $14 \leq k \leq 20$ ).

$IFR_{\sigma,k}^S$ -values among evolutionary closely related species, as Homo sapiens, Pan paniscus and Anolis carolinensis are small. However, comparing taxa, less related in the phylogenetic tree of life, the difference becomes significant. Statistical tests (two tailed Wilcoxon rank sum test) are conducted to quantify the statistical significance of this difference within the let-7 genes  $IFR_{\sigma,k}^S$ -value distribution among these six taxa, see Figure 6, for  $k = 1, 5, 20$ .

The results of statistical tests at  $k=1,5,20$  demonstrate that  $IFR_{\sigma,k}^S$ -distributions of the six taxa reflect the complexity of the organisms and their phylogenetic relations. Homo sapiens, Pan paniscus and Anolis carolinensis almost always exhibit significantly higher  $IFR_{\sigma,k}^S$ -values than Drosophila and Chromadorae, for  $k=1,5,20$ . On the other hand, differences among Homo sapiens, Pan paniscus and Anolis carolinensis are statistically insignificant for  $k=1,5,20$ . However, we observe, for  $k=20$  insignificant differences between Homo sapiens, Pan paniscus and Anolis carolinensis with Drosophila, though the  $p$  values are very close to 0.05. A more distinguished variation is observed comparing Ciona with Drosophila. In case of  $k=1$ , the difference is close of being significant with  $p=0.0554$ , but for  $k=20$ , the difference is insignificant with  $p=0.5417$ .

We proceed by conducting the above analysis for all 401 let-7 sequence-structure pairs of the miRBase. Let-7 genes have been found in 82 metazoan species. Multiple homologous miRNA genes are commonly observed in vertebrates, while single miRNA let-7 genes were more common in other animal species. The phylogenetic tree of all 82 species is constructed using the “Interactive Tree Of Life” (iTOL) (34, 35), based on NCBI Taxonomy (36). In addition, iTOL determines taxonomic classes of all internal nodes. Given the phylogenetic tree, we not only compute the mean  $IFR_{\sigma,k}^S$ -values of the let-7 sequence-structure pairs within each specific species, but also the mean  $IFR_{\sigma,k}^S$ -values within taxa, corresponding to the internal nodes of the phylogenetic tree. Figure 7 depicts a subtree of the phylogenetic tree, that includes the major taxa as well as the mean  $IFR_{\sigma,k}^S$ -values within each taxon, for  $k=1,5,20$ . The complete phylogenetic tree is presented in the SM (Figure 3,4,5).

For let-7 miRNAs, we observe that higher metazoan species typically exhibit higher  $IFR_{\sigma,k}^S$ -values as well as significant differences in the  $IFR_{\sigma,k}^S$ -distribution across taxa. For instance,  $IFR_{\sigma,k}^S$ -distributions of Deuterostomia and Protostomia are found to be significantly different ( $p=0.00016, 0.00058, 0.00033$  for  $k=1,5,20$ , calculated by two tailed Wilcoxon rank sum tests).

## DISCUSSION

In this paper we augment the analysis of genetic sequences by incorporating structural information. The information represented by structures is distinctively different from

**Table 3.** Mean  $IFR_{\sigma,k}^S$  within each taxa at each  $k$

	$k=1$	$k=5$	$k=20$
Homo sapiens	0.9288	0.6632	0.3356
Pan paniscus	0.9234	0.6404	0.3402
Anolis carolinensis	0.9211	0.6412	0.2949
Ciona	0.8874	0.5509	0.1971
Drosophila	0.8524	0.4889	0.1802
Chromadorae	0.9118	0.7904	0.0642

The table displays the mean value of  $IFR_{\sigma,k}^S$  of the let-7 sequence-structure pairs within each taxa, at  $k=1,5,20$ .

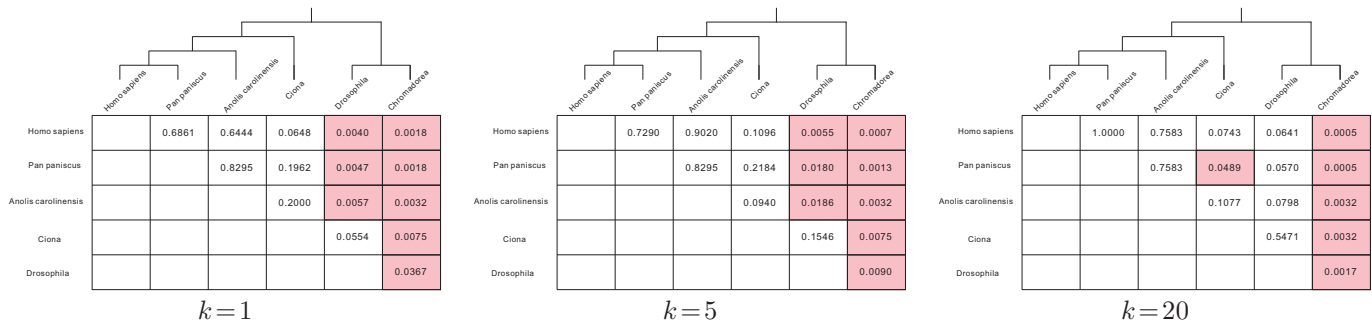


**Figure 6.** Statistical significance ( $p$  value) of the difference within the let-7 genes  $IFR_{\sigma,k}^S$ -distribution between taxa, for  $k=1$  (left),  $k=5$  (middle) and  $k=20$  (right).  $p$  values denote the probability of observing a larger difference in  $IFR_{\sigma,k}^S$ -distribution between two corresponding taxa at random, assuming they are drawn from the same probability distribution, computed by two tailed Wilcoxon rank sum test. Differences between two taxa, that are statistically significant ( $p < 0.05$ ), are highlighted and phylogenetic relations among the six taxa are displayed.

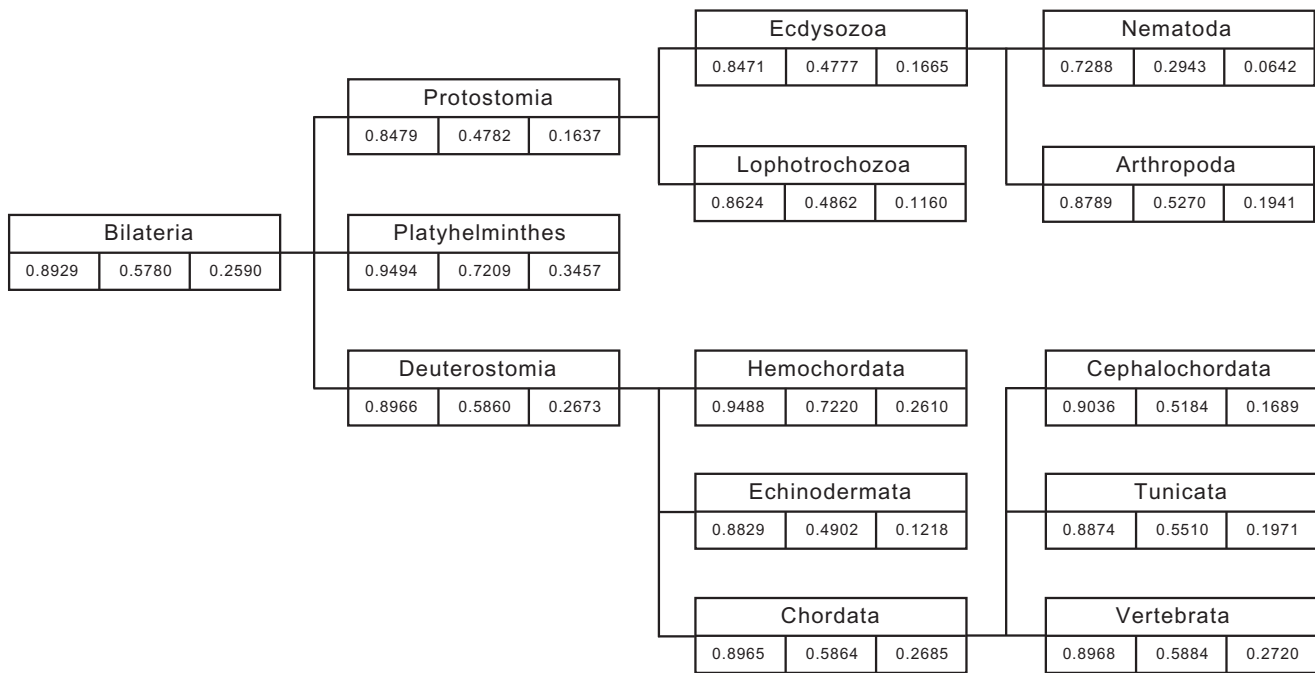


**Figure 7.** Phylogenetic tree of the major taxa and mean  $IFR_{\sigma,k}^S$  of the let-7 sequence-structure pairs within each taxon, for  $k=1, 5, 20$ . Mean  $IFR_{\sigma,k}^S$ -value for  $k=1$  (Right hand side),  $k=5$  (Center) and  $k=20$  (Left hand side).

that represented by sequences. Structures encode relations between pairs of *loci*. Such a relation can be realized in multiple ways, i.e., by the bond between loci  $i$  and  $j$  by AU, UA, GU, UG, CG and GC. In that, one can expect a meaningful enhancement of the sequence information.

Incorporating structural information, i.e. considering sequences and structures combined, provides new ways to analyze genetic material. We investigate mutational robustness of let-7 miRNA, making use of this perspective and introduce the  $IFR_{\sigma,k}^S$ -spectrum, a novel observable, that quantifies mutational robustness. The  $IFR_{\sigma,k}^S$ -spectrum depends on both: the reference sequence and structure, respectively and allows us to delocalize the study of mutational robustness beyond single-point mutations.

Our study provides evidence for direct evolution of increased robustness in let-7 miRNAs, by comparing native let-7 miRNA sequence-structure pairs with the control pairs obtained by inverse folding algorithms. It provides evidence that mutational robustness is not local, i.e. it cannot be deduced from or restricted to single-point mutations. On the contrary, robustness effects become more pronounced in higher Hamming distances: the percentage of significantly  $k$ -robust, native let-7 sequence-structure pairs increases as the Hamming distance  $k$  increases. By conducting a correlation analysis between  $IFR_{\sigma,k}^S$ -values, we provide evidence that there exist additional factors that contribute to mutational robustness against multiple-point mutations. The spectrum itself contains information that cannot be inferred from a local analysis.

The pronounced mutational robustness of native let-7 sequence-structure pairs against multiple-point mutations might play a role in genetic robustness on a population level. The presence of native sequences in a population allows for significant sequence variation within a species while still preserving the phenotype. This would suggest that evolution is not identifying sequences that are locally robust but robust within entire regions of sequence space.

An evolutionary analysis of the  $IFR_{\sigma,k}^S$ -spectrum of let-7 miRNAs shows that the  $IFR_{\sigma,k}^S$ -spectrum resembles phylogenetic relationships. Statistical tests exhibit, that closely related species tend to have similar  $IFR_{\sigma,k}^S$ -spectra while distant species tend to exhibit distinct  $IFR_{\sigma,k}^S$ -spectra. In general, higher level animal species have larger  $IFR_{\sigma,k}^S$ -values than lower level animal species. The increased mutational robustness in higher level animals appears to reflect the complexity of the organisms.

The role of structure in the context of the  $IFR_{\sigma,k}^S$ -spectrum, differs substantially from the role of neutrality in (4): structure is not merely used to measure the effect of the mutation, but also affects how sequences mutate. This constitutes effectively a feed-back loop between sequence and structure and is arguably the driving factor enhancing the signal in native sequence-structure pairs.

We use a discrete metric for measuring the structural change induced by mutation in the definition of  $IFR_{\sigma,k}^S$ -spectrum, instead of the base pair distance. This metric produces stable data: the standard error of  $IFR_{\sigma,k}^S$  by sampling 5000 times is small,  $\pm 0.0065$ , compared to the difference of  $IFR_{\sigma,k}^S$ -spectra between native and control sequence-structure pairs and the difference of  $IFR_{\sigma,k}^S$ -spectra across species, respectively. This allows us to analyze efficiently mutational robustness against multiple-point mutations by Boltzmann sampling, obsoleting the need for large sample sizes.

In our analysis, we use the MFE structures, predicted by RNA minimum free-energy folding algorithm, as phenotypes. The study can be enhanced by passing from MFE structures to partition functions of structures with respect to a fixed sequence (27). One can envision an analysis that considers the both: the dual partition function, considered here and in addition the partition function of structures.

Traditionally, the “information” of a sequence is being identified with its actual sequence of nucleotides. This perspective results in employing sequence alignments to quantify sequence similarities, the underline assumption being, that similar sequences should have close biological relevant. This however is not entirely correct. Fontana *et al.* (37) study the ruggedness of genotype to phenotype maps and show that similar sequences can exhibit distinctly different phenotype. Furthermore, in the context of sequence design and detection of new functional genes, sequences that fold into the same structure are considered to be equal (14, 38). The presence of neutral networks (39, 40, 41) of RNA secondary structures, shows, that there are complimentary sequences that fold into the same structure. In other words, neither does sequence similarity necessarily imply phenotypic similarity nor does sequence dissimilarity

imply phenotypic dissimilarity. This motivates to augment the sequence information by incorporating additional factors.

The analysis of  $IFR_{\sigma,k}^S$ -spectra represents such an augmentation: the let-7 sequences-structure pairs exhibit a distinctive difference between native and random pairs. As a result, integrating the information of sequences and structures facilitates at minimum the extension of the local analysis conducted in (4) and may as well, as a novel paradigm alone, lead to further biological insights.

## FUNDING

This research is partially funded by Thermo Fisher and the last author is a Thermo Fisher Scientific Fellow in Advanced Systems for Information Biology.

## ACKNOWLEDGEMENTS

Special thanks to Stanley Hefta for his input on this manuscript. We gratefully acknowledge the help of Kevin Shinpaugh and the computational support team at BI, Mia Shu, Thomas Li, Henning Mortveit, Madhav Marathe and Reza Rezazadegan for discussions. The fourth author is a Thermo Fisher Scientific Fellow in Advanced Systems for Information Biology and acknowledges their support of this work.

*Conflict of interest statement.* None declared.

## REFERENCES

- Gu, Z., Steinmetz, L. M., Gu, X., Scharfe, C., et al. (2003) Role of duplicate genes in genetic robustness against null mutations. *Nature*, **421**(6918), 63.
- de Visser, J. A. G. M., Hermisson, J., Wagner, G. P., Meyers, L. A., Bagheri-Chaichian, H., Blanchard, J. L., Chao, L., Cheverud, J. M., Elena, S. F., Fontana, W., et al. (2003) Perspective: evolution and detection of genetic robustness. *Evolution*, **57**(9), 1959–1972.
- Schlichting, C. D., Pigliucci, M., et al. (1998) Phenotypic evolution: a reaction norm perspective., Sinauer Associates Incorporated, .
- Borenstein, E. and Ruppin, E. (2006) Direct evolution of genetic robustness in microRNA. *Proceedings of the National Academy of Sciences*, **103**(17), 6593–6598.
- Rodrigo, G. and Fares, M. A. (2012) Describing the structural robustness landscape of bacterial small RNAs. *BMC evolutionary biology*, **12**(1), 52.
- Darnell, J. E. (2011) RNA: life’s indispensable molecule, Cold Spring Harbor Laboratory Press, .
- Breaker, R. R. (1996) Are engineered proteins getting competition from RNA?. *Current Opinion in Biotechnology*, **7**(4), 442–448.
- Serganov, A. and Patel, D. J. (2007) Ribozymes, riboswitches and beyond: regulation of gene expression without proteins. *Nature reviews. Genetics*, **8**(10), 776.
- Breaker, R. R. and Joyce, G. F. (1994) Inventing and improving ribozyme function: rational design versus iterative selection methods. *Trends in biotechnology*, **12**(7), 268–275.
- Waterman, M. S. (1978) Secondary structure of single-stranded nucleic acids. *Adv. Math. (Suppl. Studies)*, **1**, 167–212.
- Mathews, D., Sabina, J., Zuker, M., and Turner, D. (1999) Expanded sequence dependence of thermodynamic parameters improves prediction of RNA secondary structure. *J. Mol. Biol.*, **288**, 911–940.
- Zuker, M. and Stiegler, P. (1981) Optimal computer folding of larger RNA sequences using thermodynamics and auxiliary information. *Nucleic Acids Res.*, **9**, 133–148.
- Hofacker, I. L., Fontana, W., Stadler, P. F., Bonhoeffer, L. S., Tacker, M., and Schuster, P. (1994) Fast Folding and Comparison of RNA Secondary Structures. *Monatsh. Chem.*, **125**, 167–188.

14. Lorenz, R., Bernhart, S. H., Zu Siederdisen, C. H., Tafer, H., Flamm, C., Stadler, P. F., and Hofacker, I. L. (2011) ViennaRNA Package 2.0. *Algorithms for Molecular Biology*, **6**(1), 26.
15. Gruber, A. R., Bernhart, S. H., Hofacker, I. L., and Washietl, S. (2008) Strategies for measuring evolutionary conservation of RNA secondary structures. *BMC bioinformatics*, **9**(1), 122.
16. Kimura, M. (1983) The neutral theory of molecular evolution, Cambridge University Press, .
17. Mimouni, N. K., Lyngsø, R. B., Griffiths-Jones, S., and Hein, J. (2008) An analysis of structural influences on selection in RNA genes. *Molecular biology and evolution*, **26**(1), 209–216.
18. Price, N., Cartwright, R. A., Sabath, N., Graur, D., and Azevedo, R. B. (2011) Neutral evolution of robustness in Drosophila microRNA precursors. *Molecular biology and evolution*, **28**(7), 2115–2123.
19. Pollard, K. S., Salama, S. R., Lambert, N., Lambot, M.-A., Coppens, S., Pedersen, J. S., Katzman, S., King, B., Onodera, C., Siepel, A., et al. (2006) An RNA gene expressed during cortical development evolved rapidly in humans. *Nature*, **443**(7108), 167–172.
20. Beniaminov, A., Westhof, E., and Krol, A. (2008) Distinctive structures between chimpanzee and humanin a brain noncoding RNA. *RNA*, **14**(7), 1270–1275.
21. Pollard, K. S., Salama, S. R., King, B., Kern, A. D., Dreszer, T., Katzman, S., Siepel, A., Pedersen, J. S., Bejerano, G., Baertsch, R., et al. (2006) Forces shaping the fastest evolving regions in the human genome. *PLoS genetics*, **2**(10), e168.
22. Barrett, C., Huang, F. W., and Reidys, C. M. (2017) Sequence–structure relations of biopolymers. *Bioinformatics*, **33**(3), 382–389.
23. Lee, R. C., Feinbaum, R. L., and Ambros, V. (1993) The C. elegans heterochronic gene lin-4 encodes small RNAs with antisense complementarity to lin-14. *Cell*, **75**(5), 843–854.
24. Tanzer, A. and Stadler, P. F. (2004) Molecular evolution of a microRNA cluster. *Journal of molecular biology*, **339**(2), 327–335.
25. Nussinov, R., Piecznik, G., Griggs, J. R., and Kleitman, D. J. (1978) Algorithms for Loop Matching. *SIAM J. Appl. Math.*, **35**(1), 68–82.
26. Turner, D. and Mathews, D. H. (2010) NNDB: the nearest neighbor parameter database for predicting stability of nucleic acid secondary structure. *Nucl. Acids Res.*, **38**(Database), 280–282.
27. McCaskill, J. S. (1990) The equilibrium partition function and base pair binding probabilities for RNA secondary structure. *Biopolymers*, **29**(6-7), 1105–1119.
28. Huang, F. W., He, Q., Barrett, C., and Reidys, C. M. (2017) An efficient dual sampling algorithm with Hamming distance filtration. *arXiv preprint arXiv:1711.10549*,.
29. Kozomara, A. and Griffiths-Jones, S. (2013) miRBase: annotating high confidence microRNAs using deep sequencing data. *Nucleic acids research*, **42**(D1), D68–D73.
30. Garcia-Martin, J. A., Bayegan, A. H., Dotu, I., and Clote, P. (2016) RNADualPF: software to compute the dual partition function with sample applications in molecular evolution theory. *BMC bioinformatics*, **17**(1), 424.
31. Levin, A., Lis, M., Ponty, Y., O’Donnell, C. W., Devadas, S., Berger, B., and Waldspühl, J. (2012) A global sampling approach to designing and reengineering RNA secondary structures. *Nucleic acids research*, **40**(20), 10041–10052.
32. Bonnet, E., Wuyts, J., Rouzé, P., and Van de Peer, Y. (2004) Evidence that microRNA precursors, unlike other non-coding RNAs, have lower folding free energies than random sequences. *Bioinformatics*, **20**(17), 2911–2917.
33. Freilich, S., Kreimer, A., Borenstein, E., Gophna, U., Sharan, R., and Ruppín, E. (2010) Decoupling environment-dependent and independent genetic robustness across bacterial species. *PLoS computational biology*, **6**(2), e1000690.
34. Letunic, I. and Bork, P. (2006) Interactive Tree Of Life (iTOL): an online tool for phylogenetic tree display and annotation. *Bioinformatics*, **23**(1), 127–128.
35. Letunic, I. and Bork, P. (2016) Interactive tree of life (iTOL) v3: an online tool for the display and annotation of phylogenetic and other trees. *Nucleic acids research*, **44**(W1), W242–W245.
36. Federhen, S. (2011) The NCBI taxonomy database. *Nucleic acids research*, **40**(D1), D136–D143.
37. Huynen, M. A., Stadler, P. F., and Fontana, W. (1996) Smoothness within ruggedness: the role of neutrality in adaptation. *Proceedings of the National Academy of Sciences*, **93**(1), 397–401.
38. Busch, A. and Backofen, R. (2006) INFO-RNA? a fast approach to inverse RNA folding. *Bioinformatics*, **22**(15), 1823–1831.
39. Reidys, C. M., Stadler, P. F., and Schuster, P. (1997) Generic properties of combinatory maps and neutral networks of RNA secondary structures. *Bull. Math. Biol.*, **59**(2), 339–397.
40. Grüner, R., Giegerich, R., Strothmann, D., Reidys, C. M., Weber, J., Hofacker, I. L., Stadler, P. F., and Schuster, P. (1996) Analysis of RNA sequence structure maps by exhaustive enumeration I. structures of neutral networks and shape space covering.. *Chem. Mon.*, **127**, 355–374.
41. Grüner, R., Giegerich, R., Strothmann, D., Reidys, C. M., Weber, J., Hofacker, I. L., Stadler, P. F., and Schuster, P. (1996) Analysis of RNA sequence structure maps by exhaustive enumeration II. structures of neutral networks and shape space covering.. *Chem. Mon.*, **127**, 375–389.